









Spatial self-organization of vegetation in water-limited systems: mechanistic causes, empirical tests, and ecosystem-level consequences

Ricardo Martínez-García^{1,*} , ¹  ²  ³  ^{4,5}  ⁶  ^{6,†}  ^{2,†} 

¹ ICTP South American Institute for Fundamental Research & Instituto de Física Teórica - Universidade Estadual Paulista, Rua Dr. Bento Teobaldo Ferraz 271, Bloco 2 - Barra Funda 01140-070 São Paulo, SP Brazil;

² Department of Ecology and Evolutionary Biology, Princeton University, Princeton, New Jersey, United States of America;

³ Department of Ecology, Evolution, and Natural Resources, Rutgers University, New Brunswick, 08901 NJ (USA)

⁴ Center for Advanced Systems Understanding (CASUS), Görlitz, Germany;

⁵ Helmholtz-Zentrum Dresden Rossendorf (HZDR), Dresden, Germany;

⁶ Department of Ecological Modelling, Helmholtz Centre for Environmental Research – UFZ, Leipzig, Germany;

⁷ IFISC, Instituto de Física Interdisciplinar y Sistemas Complejos (CSIC-UIB), E-07122 Palma de Mallorca, Spain.

* Correspondence: ricardom@ictp-saifr.org

† These authors contributed equally to this work

Received: date; Accepted: date; Published: date

Abstract: Self-organized spatial patterns of vegetation are frequent in water-limited regions and have been suggested as important ecosystem health indicators. However, the mechanisms underlying their formation remain unclear. It has been hypothesized that patterns could emerge from a water-mediated scale-dependent feedback (SDF), whereby interactions favoring plant growth dominate at short distances while growth-inhibitory interactions dominate in the long range. As precipitation declines, this framework predicts a sequential change from gapped to labyrinthine to spotted spatial patterns. However, we know little about how net plant-to-plant interactions may shift from positive to negative as a function of inter-individual distance, and in the absence of strong empirical support, the relevance of SDF for vegetation pattern formation remains disputed. Alternative theories show that the same sequence of patterns could emerge even if net interactions between plants are always inhibitory, provided that their intensity decays sharply enough with inter-individual distance. Importantly, although these alternative hypotheses lead to visually indistinguishable spatial distributions of plants, the two different frameworks predict different ecosystem-level consequences for these resulting patterns, thus limiting their potential use as ecosystem-state indicators. Moreover, the interaction of vegetation with other ecosystem components can alter the dynamics of the pattern or even introduce additional spatio-temporal scales. Therefore, to make reliable ecological predictions, models need to accurately capture the mechanisms at play in the systems of interest. Here, we review existing theories for vegetation self-organization and their conflicting ecosystem-level predictions. We further discuss possible ways for reconciling these predictions. We focus on the mechanistic differences among models, which can provide valuable information to help researchers decide which model to use for a particular system and/or whether it requires modification.

Keywords: Water-limited ecosystems, partial differential equations, ecological patterns, reaction-diffusion systems, nonlocal models, scale-dependent feedback, Turing patterns.

Contents

1	Introduction	2
2	Ecological rationale behind models for vegetation spatial self-organization	4
3	Review of models for vegetation self-organization	5
3.1	Water-mediated scale-dependent feedbacks. The Turing principle applied to vegetation self-organization.	5
3.1.1	Two-equation water-vegetation dynamics: the generalized Klausmeier model	8
3.1.2	Three-equation water-vegetation dynamics: the Rietkerk model	8
3.2	Scale-dependent feedback kernel-based models	10
3.2.1	Models with linear nonlocal interactions	10
3.2.2	Models with nonlinear nonlocal interactions	11
3.3	Purely competitive models for vegetation spatial self-organization.	12
3.3.1	Models with linear nonlocal interactions	12
3.3.2	Models with nonlinear nonlocal interactions	13
3.3.3	Comparison between PC models with linear nonlocal interactions and PC models with nonlinear nonlocal interactions.	14
4	Self-organized patterns as indicators of ecological transitions	15
5	Testing models for vegetation self-organization in the field	17
6	Conclusions and future lines of research	19
	References	21

1. Introduction

Self-organized patterns are ubiquitous in complex biological systems. These regular structures, which can cover large portions of the system, emerge due to many nonlinear interactions among system components. Examples can be found at any spatiotemporal scale, from microbial colonies [1–3], to entire landscapes [4,5], and both in motile and in sessile organisms [6–8]. Importantly, because harsh environmental conditions provide a context in which self-organization becomes important, self-organized patterns contain important information about physical and biological processes that occur in the systems in which they form [9].

A well-known example of self-organization in ecology is vegetation pattern formation in water-limited regions [10,11]. Despite forming in very different conditions, both biotic (vegetation species, presence of different types of fauna) and abiotic (soil type, seasonality, levels of rainfall), these patterns consistently show the same shapes: vegetation spots overdispersed on a matrix of bare soil, soil-vegetation labyrinths, and gaps of bare soil overdispersed on a homogeneous layer of vegetation (see [4,10,12] for a global compilation of pattern locations). Importantly, ecosystem water availability strongly determines the specific shape of the pattern. A Fourier-based analysis of satellite imagery covering extensive areas of Sudan revealed that more humid regions are dominated by gapped patterns, whereas spotted patterns dominate in more arid conditions [13], in agreement with model predictions [14,15]. However, imagery

time series are not long enough to observe whether vegetation cover in a specific region undergoes these transitions between patterns in response to growing aridity.

After the spotted pattern, models predict that patterned ecosystems undergo a transition to a desert state if precipitation continues to decrease. The observed correlation between pattern shape and water availability suggests that the spotted pattern could serve as a reliable and easy-to-identify early-warning indicator of this ecosystem shift [16–20]. This has reinforced the motivation to develop several models aiming to explain both the formation of spatial patterns of vegetation and their dependence on environmental variables [12,14,21–24]. Although Bastiaansen *et al.* [25] has recently tested some model predictions using satellite imagery, theoretical studies using models remain the dominant approach to study this hypothesized transition.

Spatially-explicit models of vegetation dynamics fall into two main categories. Individual-based models (IBM) describe each plant as a discrete entity whose attributes change in time following a stochastic updating rule [26–28]. Continuum models describe vegetation biomass and water concentration as continuous fields that change in space and time following a system of deterministic partial differential equations (PDEMs) [29,30]. Because they incorporate much more detail than PDEMs, IBMs require computationally intensive numerical simulations, which makes it difficult to extract general conclusions about the fundamental mechanisms that drive the emergence of population-level behaviors and patterns (but see [31–39] for examples of discrete models and analytical tools to solve them). PDEMs, in contrast, neglect most of the details incorporated by IBMs, which makes them analytically tractable as spatially-extended dynamical systems [29,40]. IBMs and PDEMs thus constitute complementary approaches to study spatial vegetation dynamics: the former allow for more quantitative, system-specific predictions, whereas the latter provide more general insights into vegetation pattern formation and their ecological implications if they include the right set of mechanisms. Because here we are interested in the general features of self-organized vegetation dynamics, we focus on PDEMs and discuss how IBMs may inform improved PDEMs.

We review different families of models, discussing how spatial patterns of vegetation emerge and their predictions for the ecosystem-level consequences of the patterns. From a mathematical point of view, we can group PDEMs vegetation models into two main classes: (i) Turing-like models that use a system of PDEs [41] to describe the coupled dynamics of water and plants, and (ii) kernel-based models that describe the dynamics of the vegetation using a single partial integrodifferential equation in which the net interaction between plants is coded in a kernel function [12]. Regardless of their mathematical structure, we will refer to models accounting for both positive and negative feedbacks as *scale-dependent feedback* (SDF) models. On the other hand, we will refer to all models in which only negative feedbacks are considered as *purely competitive* (PC). Models within each of these two classes will range from the simplest ones that capture the two different mechanisms, to the more complex, which include additional processes such as two competing species of plants [42], interactions between vegetation and fauna [43,44], soil-vegetation feedbacks [45–48], landscape topography [49], and different sources of variability, including both environmental [50–56] and demographic [57,58].

Significantly, although all these models successfully reproduce the sequence of gapped, labyrinthine, and spotted patterns found in satellite imagery, they disagree in their predictions regarding the nature of the desertification transition that follows the spotted pattern. Rietkerk *et al.* [21], for instance, developed an SDF model for vegetation biomass, soil moisture, and surface water and showed that ecosystems may undergo abrupt desertification, including a hysteresis loop, following the spotted pattern. von Hardenberg *et al.* [14] used a different SDF model that only accounts for groundwater and vegetation biomass dynamics and predicted abrupt desertification following the spotted pattern. However, they also found multistability between patterned states, i.e., for fixed environmental conditions, the shape of the stationary pattern depends on the initial state. Finally, Martínez-García *et al.* [59] developed a family of purely competitive

models in which desertification occurs gradually with progressive loss of vegetation biomass. The nature of this transition has significant ecological consequences. Abrupt transitions like those predicted by Rietkerk *et al.* [21] and von Hardenberg *et al.* [14] are almost irreversible, entail hysteresis, and due to their catastrophic and abrupt character, are difficult to prevent. Continuous transitions, however, are much easier to predict and, therefore, to manage. Determining whether ecosystems will respond abruptly or gradually to aridification is critical both from an ecosystem-management and socio-economic point of view because water-limited ecosystems cover 40% of Earth's land surface and are home to 35% of the world population [60].

Active lines of theoretical research have focused on understanding how different components of the ecosystem may interact with each other to determine an ecosystem's response to aridification [46], as well as on designing synthetic feedbacks (in the form of artificial microbiomes) that could prevent or smooth ecosystem collapses [61–63]. The question has also attracted considerable attention from empirical researchers [64]. Whether desertification is more likely to occur gradually or abruptly remains largely unknown, despite evidence suggesting that certain structural and functional ecosystem attributes respond abruptly to aridity [65].

Here, we outline and rank strategies to answer this question. In section 2, we discuss the ecological rationale behind PDEMs for vegetation self-organization. In section 3, we review different families of PDEMs for vegetation self-organization. Next, in section 4, we show that, although all lead to seemingly identical patterns, different models predict very different transitions into the desert state, limiting the reliability of model predictions regarding how or when the transition will occur and the underlying mechanisms. In section 5, we discuss possible manipulative experiments and empirical measures that could support or discard each of the previously scrutinized models. Finally, in section 6, we envision different research lines that build on these results and discuss how to apply lessons learned from studying self-organized vegetation patterns to other self-organizing biological and physical systems.

2. Ecological rationale behind models for vegetation spatial self-organization

Models of spatial self-organization of vegetation rely on simple ecological assumptions about the scale-dependence of the net biotic interaction among individual plants. That is, about the effect that the presence of one individual has on the growth and survival of its neighbors as a function of the inter-individual distance. However, this net effect is a simplification, and the mechanisms underpinning the net interaction between individuals can be very complex [66]. In the case of vegetation, such mechanisms are based on the biophysical effects of the plant canopy on the microclimate underneath and of the root system on the soil conditions (Fig. 1a). While some of these mechanisms are well studied by ecologists, we know little about how they scale with the distance between individual (or clumps of) plants, making existing models hard to parameterize using empirical observations.

The rationale behind scale-dependent feedbacks is diverse and based on different empirical observations. For example, in semiarid and arid open-canopy systems, where the range of the root system is larger than the canopy cover, the positive effects of shade can overcome competition for light and even be stronger than the effects of root competition, thereby leading to under-canopy facilitation [67]. In this context, focal plants have an overall facilitative effect in the area of most intense shade at the center of the crown, which progressively loses intensity and vanishes as shading disappears and gives rise to simple below-ground competition in areas farther from the plant (Fig. 1b). A different rationale is necessary for models in which the net biotic interaction emerges from the competition between plants for water or, more specifically, from the capacity that plants have to modify soil structure and porosity, and therefore enhance soil water infiltration [68]. Enhanced water infiltration has a direct positive effect near the plant because it increases soil water content but, as a by-product, it has negative consequences farther

away from its insertion point because, by increasing local infiltration, plants also reduce the amount of water that can infiltrate further away in plant-less bare soil locations [69,70]. Spatial heterogeneity in water availability due to plant-enhanced infiltration is higher in sloped terrains where runoff water happens exclusively down-slope (Fig. 1c), but it can be assumed in flat landscapes as well [14,41]. If runoff water is very fast and plants facilitate infiltration substantially, plants will deplete water in their surrounding bare soil areas, even beyond the range of their root system [21]. Slope-mediated dynamics result in a SDF similar to the one emerging from the interplay between canopy shading effects and root-mediated competition for resources, but at a larger scale (Fig. 1c).

However, these assumed complex combinations of biophysical mechanisms often lack reliable empirical support and might vary from system to system. For example, Trautz *et al.* [71] measured an SDF with short-range competition and long-range facilitation. Moreover, no empirical study has yet shown that a specific SDF leads to vegetation patterns. In contrast, competition is a ubiquitous interaction mechanism that affects the relation between any two plants that are located in sufficient proximity. Above-ground, plants compete for light through their canopies; below-ground, they compete for several soil resources, including water and nitrogen, through their roots [72]. If we assume, as PC models do, that only competitive mechanisms occur, we should expect plants to compete within a specific spatial range set by their physical reach, either the span of the roots or the extent of the canopy (Fig. 1d). Long but finite-range competition is the only interaction required by PC models to explain vegetation self-organization. PC models are hence the most parsimonious class of models that generates observed vegetation patterns, which makes them easier to test empirically than SDF models (see section 5).

In the next section, we review the mathematical basis of SDF and PC models. We start with models for water-mediated SDFs in section 3.1. Then, we move to kernel-based models, starting with SDF models in section 3.2) and continuing with PC models in section 3.3.

3. Review of models for vegetation self-organization

3.1. Water-mediated scale-dependent feedbacks. The Turing principle applied to vegetation self-organization.

In 1952, Turing showed that differences in the diffusion coefficients of two reacting substances can lead to the formation of stable spatial heterogeneities in their concentration [73]. In Turing's original model, one of the chemicals acts as an activator and produces both the second chemical and more of itself via an autocatalytic reaction. The second substance inhibits the production of the activator and therefore balances its concentration (see Fig. 2a for a diagram of this reaction). Spatial heterogeneities can emerge around a stationary balance of chemical concentrations if it is stable to non-spatial perturbations but unstable against spatial perturbations. This means that the homogeneous equilibrium reached in the absence of diffusion is locally stable, but destabilizes in the presence of diffusion. For this to occur, the difference between the diffusion coefficients of each substance is key. Specifically, the inhibitor must diffuse much faster than the activator, so that it inhibits the production of the activator at a long range and confines the concentration of the activator locally (see Fig. 2b for a one-dimensional sketch of how patterns emerge in a Turing activation-inhibition principle). The activation-inhibition principle responsible for pattern formation thus relies on a scale-dependent feedback: positive feedbacks (autocatalysis) dominate on short scales and negative, inhibitory feedbacks dominate on larger scales.

In the context of vegetation pattern formation, plant biomass acts as the self-replicating activator. Several positive feedbacks have been hypothesized to act as autocatalyzers of vegetation growth, such as enhanced water infiltration in the presence of plants [21,41,74] or the attraction of water towards patches of vegetation by laterally extended roots [43,75]. Water is a limiting resource and, hence, water scarcity would act as an inhibitor of vegetation growth. Negative feedbacks appear due to the lack of water far

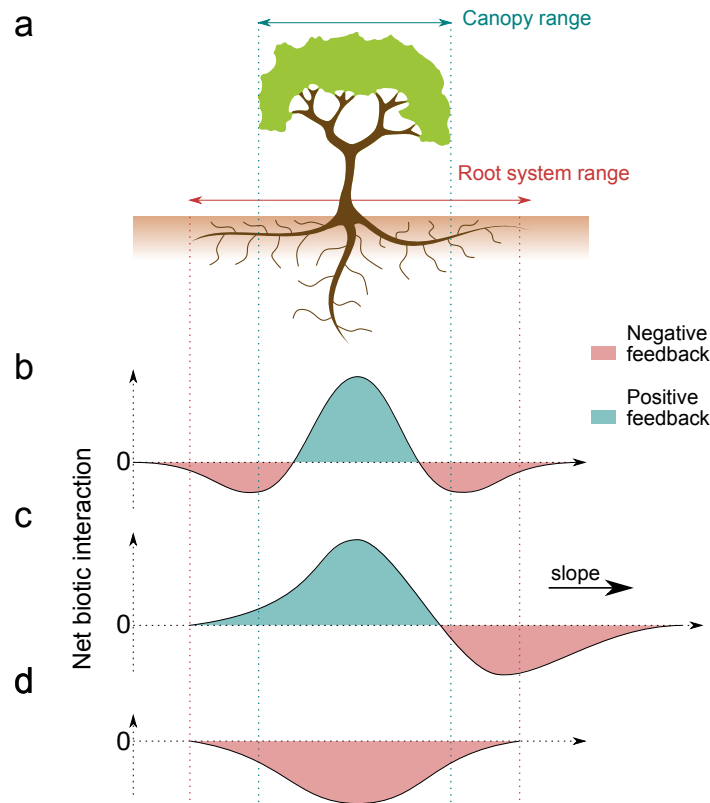


Figure 1. (a) Schematic of a plant canopy and spatial distribution of the root system. b-d) Three assumptions for the spatial variation of the net biotic interaction between a focal plant and its neighbors. b) A scale-dependent feedback with short-range facilitation and long-range competition, c) scale-dependent feedback similar to b) but in a sloped terrain, and d) a purely competitive interaction dominates the net interaction at all spatial scales.

from vegetation patches as a result of the effect of the positive feedbacks. Because plant dispersal occurs over much shorter spatial scales than water diffusion, the negative feedback has a much longer range than the positive one. In the long-term, fwater-vegetation models including these hypothesized mechanisms recover the set of gapped, labyrinthine and spotted patterns characteristic of Turing’s activation-inhibition principle (Fig. 3). Importantly, in these models, the transition between each type of pattern is controlled by precipitation intensity, a proxy for environmental conditions. Gapped patterns emerge for more humid systems and spotted patterns for more arid ones [14]. More complex transient structures, such as rings of vegetation, can be observed for certain initial conditions [22].

To discuss water-vegetation models, we will first focus on an extension of the seminal work by Klausmeier [41] that describes the interaction between water and vegetation (with densities $w(r, t)$ and $v(r, t)$, respectively) in a two-dimensional flat environment. Then, we will study a more complex model, introduced in Rietkerk *et al.* [21] that distinguishes between soil and surface water, and thus includes additional feedbacks.

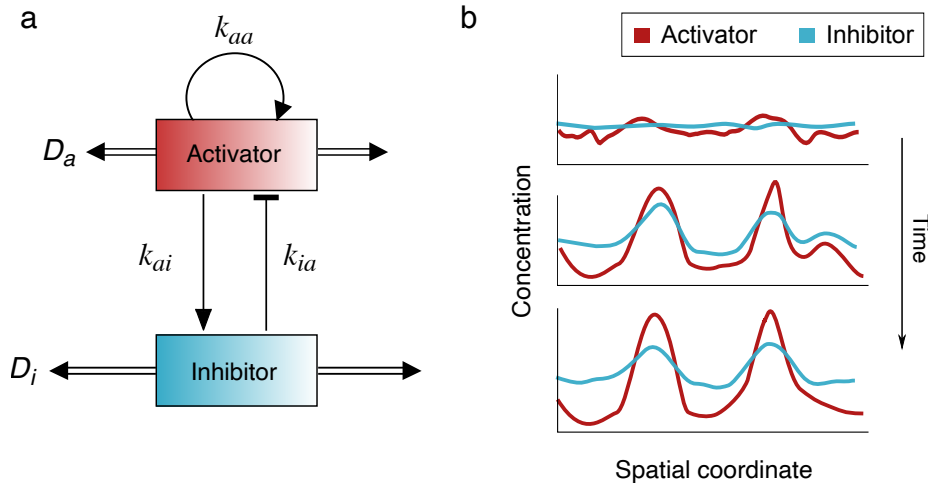


Figure 2. a) Schematic of the Turing activation-inhibition principle. The activator, with diffusion coefficient D_a , produces the inhibitor at rate K_{ai} as well as more of itself at rate K_{aa} through an autocatalytic reaction. The inhibitor degrades the activator at rate K_{ia} and diffuses at rate $D_i > D_a$. b) Schematic of the pattern-forming process in a one-dimensional system.

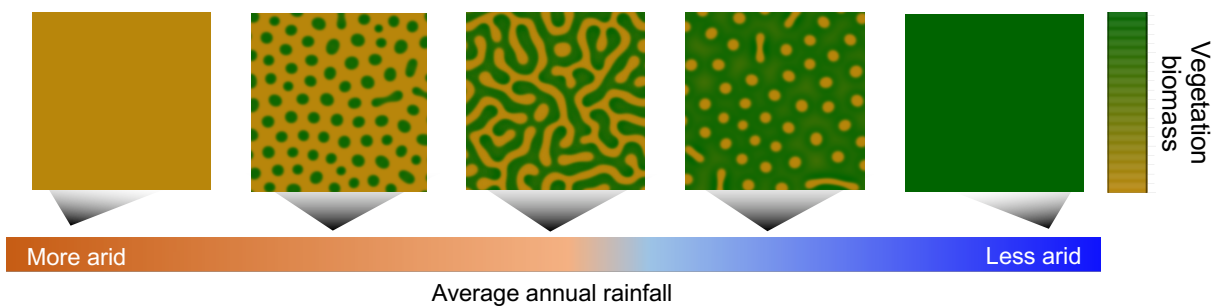


Figure 3. Schematic representation of the patterns of vegetation predicted by Turing-like models along a gradient of average annual rainfall.

3.1.1. Two-equation water-vegetation dynamics: the generalized Klausmeier model

Although it was initially formulated to describe the formation of stripes of vegetation in sloping landscapes [41], subsequent studies have extended Klausmeier's model to flat surfaces [25,56,76]. Mathematically, the generalized version of Klausmeier's model is given by the following equations:

$$\frac{\partial w(\mathbf{r}, t)}{\partial t} = R - a g(w) f(v) v(\mathbf{r}, t) - l w(\mathbf{r}, t) + D_w \nabla^2 w(\mathbf{r}, t), \quad (1)$$

$$\frac{\partial v(\mathbf{r}, t)}{\partial t} = a q g(w) f(v) v(\mathbf{r}, t) - m v(\mathbf{r}, t) + D_v \nabla^2 v(\mathbf{r}, t), \quad (2)$$

where $w(\mathbf{r}, t)$ and $v(\mathbf{r}, t)$ represent water concentration and density of vegetation biomass, respectively. In Eq. (1), water is continuously supplied at a precipitation rate R , and its concentration decreases due to physical losses such as evaporation, occurring at rate l , and local uptake by plants. Water uptake is modeled by the term $a g(w) f(v) v$, in which a is the plant absorption rate, $g(w)$ describes the dependence of vegetation growth on water availability, and $f(v)$ is an increasing function of vegetation density that represents the positive effect that the presence of plants has on water infiltration. Finally, water diffuses with a diffusion coefficient D_w . Similarly, Eq. (2) accounts for vegetation growth due to water uptake, plant mortality at rate m , and plant dispersal. In the plant growth term, the parameter q represents the yield of plant biomass per unit of consumed water. In the original model, the plant absorption rate and the response of plants to water are linear ($g(w) = w(\mathbf{r}, t)$ and $f(v) = v(\mathbf{r}, t)$) which facilitates the analytical tractability of the model. However, other biologically-plausible choices can be made for these functions in order to account for processes such as saturation in plant growth due to intraspecific competition [42].

The generalized Klausmeier model has three spatially-homogeneous equilibria, obtained from the fixed points of Eqs. (1)-(2): an unvegetated state $(0, R/l)$, stable for any value of the rainfall parameter; and two states in which vegetation and water coexist at non-zero values. Of these two, only one is stable against non-spatial perturbations, which guarantees bistability, that is, the presence of alternative stable states and hysteresis. For spatial perturbations, however, the vegetated state becomes unstable within a range of R , and the system develops spatial patterns, indicating that patterns in this model originate from a Turing instability.

3.1.2. Three-equation water-vegetation dynamics: the Rietkerk model

The Rietkerk model extends the generalized Klausmeier model by splitting Eq. (1) for water concentration in two equations: one for surface water, and another one for soil water, and including a term that represents water infiltration. Moreover, the functions that represent water uptake and infiltration are nonlinear, which makes the model mechanistic, but also more complex, with more feedbacks between vegetation, soil moisture and surface water. The model equations are as follows:

$$\frac{\partial u(\mathbf{r}, t)}{\partial t} = R - \alpha \frac{v(\mathbf{r}, t) + k_2 w_0}{v(\mathbf{r}, t) + k_2} u(\mathbf{r}, t) + D_u \nabla^2 u(\mathbf{r}, t) \quad (3)$$

$$\frac{\partial w(\mathbf{r}, t)}{\partial t} = \alpha \frac{v(\mathbf{r}, t) + k_2 w_0}{v(\mathbf{r}, t) + k_2} u(\mathbf{r}, t) - g_m \frac{v(\mathbf{r}, t) w(\mathbf{r}, t)}{k_1 + w(\mathbf{r}, t)} - \delta_w w(\mathbf{r}, t) + D_w \nabla^2 w(\mathbf{r}, t) \quad (4)$$

$$\frac{\partial v(\mathbf{r}, t)}{\partial t} = c g_m \frac{v(\mathbf{r}, t) w(\mathbf{r}, t)}{k_1 + w(\mathbf{r}, t)} - \delta_v v(\mathbf{r}, t) + D_v \nabla^2 v(\mathbf{r}, t) \quad (5)$$

where $u(\mathbf{r}, t)$, $w(\mathbf{r}, t)$, and $v(\mathbf{r}, t)$ are the density of surface water, soil water, and vegetation, respectively. In Eq. (3), R is the mean annual rainfall, providing a constant supply of water to the system; the second term accounts infiltration; and the diffusion term accounts for the lateral circulation of water on the surface. In

Eq. (4), the first term represents the infiltration of surface water into the soil, which is enhanced by the presence of plants; the second term represents water uptake; the third one accounts for physical losses of soil water, such as evaporation; and the diffusion term describes the lateral circulation of water in the soil. Finally, the first term in Eq. (5) represents vegetation growth due to the uptake of soil water, which is a function that saturates for high water concentrations; the second term accounts for biomass loss at constant rate due to natural death or external hazards; and the diffusion term accounts for plant dispersal. The meaning of each parameter in the equations, together with the values used in Rietkerk *et al.* [21] for their numerical analysis, are provided in Table 1.

In the absence of diffusion, this model allows for two different steady states: a nontrivial one in which vegetation, soil water, and surface water coexist at non-zero values; and an unvegetated (i.e., desert) state in which only soil water and surface water are non-zero. The stability of each of these states switches at $R = 1$. For $R < 1$, only the plantless equilibrium is stable against non-spatial perturbations whereas for $R > 1$ the vegetated equilibrium becomes stable and the desert state, unstable. At the bifurcation point, $R = 1$, both homogeneous equilibria are unstable against spatial perturbations, which is a signature of Turing's principle for pattern formation [73]. Through numerical simulations and based on the parameterization in Table 1, we have identified a pattern regime within the interval $0.7 \lesssim R \lesssim 1.3$, which is in agreement with analytical approximations [77]. Within this range of mean annual rainfall, the patterns sequentially transition from gaps to labyrinths to spots with increasing aridity (Fig. 3). For $R \approx 0.7$, the system transitions abruptly from the spotted pattern to the desert state.

Parameter	Symbol	Value
c	Water-biomass conversion factor	10 ($\text{g mm}^{-1} \text{m}^{-2}$)
α	Maximum infiltration rate	0.2 (day^{-1})
g_m	Maximum uptake rate	0.05 ($\text{mm g}^{-1} \text{m}^{-2} \text{day}^{-1}$)
w_0	Water infiltration in the absence of plants	0.2 (-)
k_1	Water uptake half-saturation constant	5 (mm)
k_2	Saturation constant of water infiltration	5 (g m^{-2})
δ_w	Soil water loss rate	0.2 (day^{-1})
δ_v	Plant mortality	0.25 (day^{-1})
D_w	Soil water lateral diffusivity	0.1 ($\text{m}^2 \text{day}^{-1}$)
D_v	Vegetation dispersal	0.1 ($\text{m}^2 \text{day}^{-1}$)
D_u	Surface water lateral diffusivity	100 ($\text{m}^2 \text{day}^{-1}$)

Table 1. Typical parameterization of the Rietkerk model [21].

The Rietkerk model assumes constant rainfall, homogeneous soil properties, and only local and short-range processes. Therefore, all the parameters are constant in space and time, and patterns emerge from scale-dependent feedbacks between vegetation biomass and water availability alone. This simplification of the conditions in which patterns form is, however, not valid for most ecosystems.

Arid and semi-arid regions feature seasonal variability in rainfall [78]. Kletter *et al.* [79] showed that, depending on the functional dependence between water uptake and soil moisture, stochastic rainfall might increase the amount of vegetation biomass in the ecosystem compared to a constant rainfall scenario. Moreover, the properties of the soil often change in space. A widespread cause of this heterogeneity is soil-dwelling macrofauna, such as ants, earthworms, and termites [5]. Bonachela *et al.* [46] found that heterogeneity in substrate properties induced by soil-dwelling macrofauna, and modeled by space-dependent parameters, might interact with SDFs between water and vegetation. This coupling both introduces new characteristic spatial scales in the pattern and reduces the abruptness of the transition into a desert state and its hysteresis loop, which makes the ecosystem more resistant to aridification and easier to restore. Finally, researchers have also extended the Rietkerk model to account for long-range, nonlocal

processes. For example, Gilad *et al.* [43] introduced a nonlocal mechanism in the vegetation density growth of Eqs. (3)-(5) that mimics the long-range of plant root systems. Specifically, they considered that vegetation growth at each location depends on the average density of water available within a neighbor region of the location rather than by water availability at the focal location. Similarly, they considered that water uptake at each location depends on the average density of vegetation biomass within a neighborhood centered at the location. The size of this neighborhood is a model proxy for root system extension and the averages are weighted by a kernel function that represents how the influence of each point within the neighborhood decays with distance to the focal location. It is important to note, however, that although models like the one developed in Gilad *et al.* [43] contain kernel functions, they do not rely on the shape of the kernel for the emergence of patterns, and the pattern-forming instability is still given by difference in water and vegetation diffusion rates. Therefore, we will consider the Gilad model (and modifications to it) as a Turing-like model instead of a kernel-based one.

3.2. Scale-dependent feedback kernel-based models

Kernel-based models are those in which all the water-vegetation feedbacks are encapsulated in a single nonlocal net interaction between plants. The nonlocality in the net plant interaction accounts for the fact that individual (or patches of) plants can interact with each other within a finite neighborhood. Therefore, the vegetation dynamics at any point of the space is coupled to the density of vegetation at locations within the interaction range. The specifics of this coupling, such as whether it enhances or inhibits plant growth as well as its spatial range, are contained in a kernel function whose mathematical properties determine the conditions for pattern formation. Moreover, because all water-vegetation feedbacks are collapsed into a net interaction between plants, kernel-based models do not describe the dynamics of any type of water and use a single partial integro-differential equation for the spatiotemporal dynamics of the vegetation.

Next, we discuss different families of kernel-based models, depending on how the kernel function is introduced in the equation (linearly or nonlinearly) and the nature of the net interaction it accounts for (scale-dependent feedback or purely competitive).

3.2.1. Models with linear nonlocal interactions

The first family of kernel-based models that we will discuss assumes that plants promote the proliferation of more individuals within their near neighborhood, and they inhibit the establishment of new plants in their far neighborhood. This distance-dependent switch in the sign of the interaction represents a scale-dependent feedback [12]. As explained in Section 2, the facilitation range is usually assumed to be determined by the plant crown, while the competition range is related to the lateral root length (Fig. 1a). The kernel is often defined as the addition of two Gaussian functions with different widths, with the wider function taking negative values to account for the longer range of competitive interactions [80] (Fig. 1c). Given the analogy between these kernels and the ones used to model processes such as patterns of activity in neural populations, these models are also termed neural models [81,82].

Within kernel-based SDF models, we distinguish between those in which the spatial coupling (nonlocal interactions) enters in the equations linearly [80], and those in which it enters nonlinearly [83]. In the simpler linear case, the spatial coupling is added to the local dynamics,

$$\frac{\partial v(\mathbf{r}, t)}{\partial t} = h(v) + \int d\mathbf{r}' G(\mathbf{r}'; \mathbf{r}) [v(\mathbf{r}', t) - v_0], \quad (6)$$

The first term describes the local dynamics of the vegetation, i.e., the temporal changes in vegetation density at a location \mathbf{r} due to processes in which neighboring vegetation does not play any role. The

integral term describes the spatial coupling, i.e., changes in vegetation density at \mathbf{r} due to vegetation density at neighbor locations \mathbf{r}' . v_0 represents the spatially homogeneous steady state, solution of $h(v_0) = 0$. Assuming spatial isotropy, the kernel function $G(\mathbf{r}, \mathbf{r}')$ decays radially with the distance from the focal location, $|\mathbf{r}' - \mathbf{r}|$, and it can be written as $G(\mathbf{r}', \mathbf{r}) = G(|\mathbf{r}' - \mathbf{r}|)$. Therefore the dynamics of vegetation density is governed by two main contributions: first, if spatial coupling is neglected, vegetation density increases or decreases locally depending on the sign of $h(v)$; second, the spatial coupling enhances or diminishes vegetation growth depending on the sign of the kernel function and the difference between the local vegetation density and the spatially homogeneous steady state v_0 .

Assuming kernels that are positive close to the focal location and negative far from it, local perturbations in the vegetation density around v_0 are locally enhanced if they are larger than v_0 and attenuated otherwise. As a result, the integral term destabilizes the homogeneous state when perturbed, and spatial patterns arise in the system. Long-range growth-inhibition interactions, together with nonlinear terms in the local-growth function $h(v)$, avoid the unbounded growth of perturbations and stabilize the pattern. However, although this mechanism imposes an upper bound to vegetation density, nothing prevents v from taking unrealistic, negative values. To avoid this issue, numerical integrations of Eq. (6) always include an artificial bound at $v = 0$ such that vegetation density is reset to zero whenever it becomes negative.

3.2.2. Models with nonlinear nonlocal interactions

As an alternative, modulating the spatial coupling with nonlinear terms can ensure that vegetation density is always positive. For example, the pioneering model developed by Lefever and Lejeune [83] consists of a modified Verhulst-Fisher (or logistic) type equation in which each of the terms includes an integral term to encode long-range spatial interactions,

$$\frac{\partial v(\mathbf{r}, t)}{\partial t} = \beta (\omega_1 * v)(\mathbf{r}, t) \left[1 - \frac{(\omega_2 * v)(\mathbf{r}, t)}{K} \right] - \eta (\omega_3 * v)(\mathbf{r}, t) \quad (7)$$

where β is the rate at which seeds are produced (a proxy for the number of seeds produced by each plant) and η is the rate at which vegetation biomass is lost due to spontaneous death and external hazards such as grazing, fires, or anthropogenic factors. The model assumes spatial isotropy, and the symbol $*$ indicates a linear convolution operation:

$$(\omega_i * v)(\mathbf{r}, t) = \int d\mathbf{r}' \omega_i(\mathbf{r} - \mathbf{r}'; \ell_i) v(\mathbf{r}', t) \quad (8)$$

in which each ω_i is a weighting function with a characteristic spatial scale ℓ_i that defines the size of the neighborhood contributing to the focal process. For instance, $\omega_1(\mathbf{r} - \mathbf{r}'; \ell_1)$ defines the size of the neighborhood that contributes to the growth of vegetation biomass at \mathbf{r} . Similarly, ℓ_2 defines the scale over which plants inhibit the growth of their neighbors, and ℓ_3 the scale over which vegetation density influences the spontaneous death rate of vegetation at the focal location (called *toxicity length* in Lefever and Lejeune [83]). Because the sign of the interaction is explicit in each term of Eq. (7), the convolutions only represent weighted averages of vegetation biomass and the weighting functions must be defined to be positive. Finally, Lefever and Lejeune [83] set the scale of the inhibitory interactions larger than the scale of the positive interactions ($\ell_2 > \ell_1$), and thus the model includes a SDF with short-range facilitation and long-range competition. Expanding upon this work, several other models have introduced non-linear spatial couplings via integral terms [84–86], and others have expanded the integral terms and studied the formation of localized structures of vegetation [87].

3.3. Purely competitive models for vegetation spatial self-organization.

In previous sections, we invoked the existence of SDFs in the interactions among plants to explain the emergence of self-organized spatial patterns of vegetation. However, competition and facilitation usually act simultaneously and are hard to disentangle [88]. This intricate coupling between positive and negative plant-to-plant interactions, together with the various biophysical processes that may underlie each of them, makes it difficult to understand how the net interaction between two neighbors may shift from positive to negative with the distance between them. For example, Trautz *et al.* [71] reported a scale-dependent feedback between neighboring plants in which negative interactions dominate on the short range and positive interactions dominate on the long range. Moreover, some studies have highlighted the importance of long-range negative feedbacks on pattern formation, suggesting that short-range positive feedbacks might be secondary actors that sharpen the boundaries of clusters rather than being key for the instabilities that lead to the patterns [11,89,90]. Following these arguments, Martinez-Garcia *et al.* [23,59] proposed a family of purely competitive models with the goal of identifying the smallest set of mechanisms needed for self-organized vegetation patterns to form. Specifically, the goal of these studies was to determine whether SDFs are necessary for self-organized patterns to form or if, instead, one of these two feedbacks acting alone can drive the emergence of spatial patterns of vegetation in water-limited ecosystems.

3.3.1. Models with linear nonlocal interactions

Inspired by the neural models with short-range facilitation and long-range inhibition described by Eq. (6), the simplest purely competitive models consider linear nonlocal interactions. Models in this family can be written as:

$$\frac{\partial v(\mathbf{r}, t)}{\partial t} = D \nabla^2 v(\mathbf{r}, t) + \beta v(\mathbf{r}, t) \left(1 - \frac{v(\mathbf{r}, t)}{K}\right) + \lambda \int d\mathbf{r}' G(|\mathbf{r}' - \mathbf{r}|) v(\mathbf{r}', t) \quad (9)$$

where the first term on the right side represents seed dispersal; the second term is a growth term in which the logistic-like growth-limiting factor $(1 - v/K)$ represents local competition for space, β is the seed production rate, and K the local carrying capacity; the third term accounts for long-range interactions between individuals at \mathbf{r} and their neighbors at \mathbf{r}' . $\lambda > 0$ represents the intensity of the interaction and can be seen as a proxy for resource or any other mean of intraspecific competition, and the kernel function $G(|\mathbf{r}' - \mathbf{r}|)$ is necessarily negative to account for a competitive net interaction that inhibits vegetation growth.

As in Eq. (6), there is no lower bound for v , which can take negative values due to the linear nonlocal term. Thus, an artificial bound at $v = 0$ is needed in the numerical integration of Eq. (9) to ensure ecological plausibility [12]. On the other hand, a typical choice for the kernel G is a top-hat function of $|\mathbf{r} - \mathbf{r}'|$, but a linear stability analysis of the model equation reveals that patterns may form for many other kernel shapes [23]. More specifically, a necessary condition for pattern formation is that the Fourier transform of the kernel function takes negative values for certain wavenumbers, which indicates a sharp decay in the strength of the nonlocal interactions [23,59]. Importantly, the Fourier transform of any kernel function with a discontinuity at a distance $|\mathbf{r} - \mathbf{r}'|$ takes negative values for a finite range of wavenumbers and can potentially lead to patterns. Provided that the kernel function meets this condition, the intensity of the nonlocal competition λ controls a transition to patterns, and for large values of λ , the model develops a sequence of labyrinthine and spotted patterns similar to those observed in Turing-like. Gapped patterns, however, have not been found in models in which nonlocal interactions are inhibitory and linear.

3.3.2. Models with nonlinear nonlocal interactions

Alternatively, nonlocal interactions can be represented through nonlinear functions modulating either the growth or the loss terms. In both cases, the models develop the full sequence of gapped, labyrinthine and spotted patterns. We will focus on the case in which nonlocal interactions modulate the growth term as first introduced in Martínez-García *et al.* [59] although very similar results are obtained when they modulate the death term [23]:

$$\frac{\partial v(\mathbf{r}, t)}{\partial t} = P_E(\tilde{v}, \delta) \beta v(\mathbf{r}, t) \left(1 - \frac{v(\mathbf{r}, t)}{K}\right) - \eta v(\mathbf{r}, t), \quad (10)$$

where β and K are the seed production rate and the local carrying capacity as defined in Eq. (9), δ is the competition-strength parameter, and $\tilde{v}(\mathbf{r}, t)$ is the average density of vegetation around the focal position \mathbf{r} , termed ‘nonlocal vegetation density’ in the following. Assuming spatial isotropy, this nonlocal vegetation density can be calculated as

$$\tilde{v}(\mathbf{r}, t) = \int d\mathbf{r}' \mathcal{G}(|\mathbf{r}' - \mathbf{r}|) v(\mathbf{r}', t). \quad (11)$$

where the kernel function \mathcal{G} weighs the contribution of vegetation at a location \mathbf{r}' to the nonlocal vegetation density at location \mathbf{r} and is necessarily defined positive. Because it is a weighting function, \mathcal{G} only defines a range of influence of a focal plant, typically determined by the characteristic scale of the function, q , and how this influence changes with the distance from the plant [like ω_i functions do in Eq. (7)]. The models further assumes that vegetation losses occur at constant rate η and vegetation grows through a three-step sequence of seed production, local dispersal, and establishment [36]. Mathematically, this sequence is represented by the three factors that contribute to the first term in Eq. (10). First, plants produce seeds at a constant rate β , which leads to the a growth term $\beta v(\mathbf{r}, t)$. Second, seeds disperse locally and compete for space which defines a local carrying capacity K . Third, plants compete for resources with other plants, which is modeled using a plant establishment probability, P_E . Because the only long-range interaction in the model is root-mediated interference and competition for resources is more intense in more crowded environments, P_E is a monotonically decreasing function of the nonlocal vegetation density $\tilde{v}(\mathbf{r}, t)$ defined in Eq. (11). Moreover, P_E also depends on a competition-strength parameter, δ , that represents the limitation of resources. In the limit $\delta = 0$, resources are abundant, competition is weak and $P_E = 1$. Conversely, in the limit $\delta \rightarrow \infty$, resources are very scarce, competition is very strong and therefore $P_E \rightarrow 0$.

Given the general conditions explained above, a complete description of the model needs to specify the kernel function \mathcal{G} and the functional form of the probability of establishment, P_E . However, even without fixing these two functions, one can prove the existence of patterns in Eq. (10) from general properties of P_E . As for models with linear nonlocal interactions, a necessary condition for patterns to develop is that the Fourier transform of \mathcal{G} becomes negative for at least one wavenumber. Once the kernel meets this condition, the parameter ranges for which pattern formation occurs can be derived via linear stability analysis of the homogeneous solutions of the equation [40]. This analysis was conducted in Martínez-García *et al.* [59]. For low values of the competition strength δ , a homogeneous state with $v \neq 0$ is stable and patterns do not form. However, as δ increases, the homogeneous state becomes unstable and a sequential series of gapped, labyrinthine and spotted patterns develops. A desert state, however is never reached because vegetation density tends asymptotically to zero. Using the seed production rate β as control parameter, this same sequence of gapped-labyrinthine-spotted patterns develops as β decreases. When seed production rate becomes too low, vegetated patterns cannot be sustained and the system collapses into a desert-like, unvegetated state.

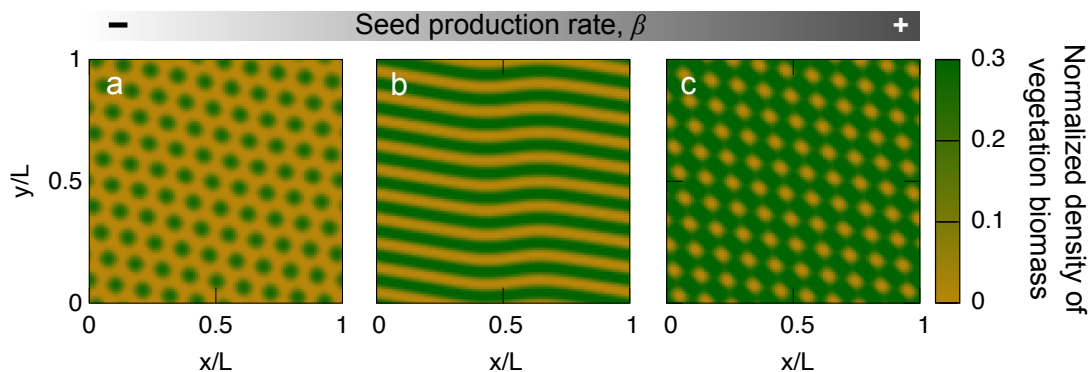


Figure 4. As seed production rate increases, which can be seen as resulting from improving environmental conditions, self-organized patterns from the purely competitive model introduced in Martínez-García *et al.* [59] transition from spotted to labyrinthine to gapped. The model is integrated on a 2D square lattice with periodic boundary conditions and using an exponential function for the seed-establishment probability $P_E = \exp(-\delta\hat{\rho})$. Simulations are started from an uncorrelated random initial condition in which the value of the vegetation density at each node of the lattice is drawn from a uniform distribution between 0 and 1. Parameterization: $\delta = 10$, $\eta = 1$ and $\beta = 2$ (panel a), $\beta = 6$ (panel b), and $\beta = 15$ (panel c).

3.3.3. Comparison between PC models with linear nonlocal interactions and PC models with nonlinear nonlocal interactions.

In the previous two sections, we discussed how linear and nonlinear implementations of nonlocal interactions in PC models result in the same sequence of patterns, which is also the same sequence obtained with SDF models. The conditions needed for patterns to emerge in PC models depend entirely on the shape of the spatial interactions. Specifically, regardless of whether nonlocal interactions are encoded linearly or nonlinearly, a necessary condition for pattern formation in PC models is that the Fourier transform of the kernel is negative for at least one wavenumber [23,59]. This condition indicates that the symmetry-breaking mechanism that triggers pattern formation is encoded in the nonlocal term, rather than in some nonlinearity in the local dynamics, thus agreeing with kernel-based SDF models [12]. For certain choices of the kernel function, small local perturbations to the homogeneous distribution of vegetation are enhanced through the formation of exclusion areas: regions of the space in which the density of roots (and therefore plant-to-plant competition) is extremely high. If two patches in which vegetation density is larger than the homogeneous stationary state are separated by a distance larger than q but smaller than $2q$, then there is not inter-patch competition because plants are separated by a distance larger than the interaction range (Fig. 5a, b). However, because the distance between patches is shorter than $2q$, there is a region halfway between both clusters in which plants compete with both patches and are thus subject to stronger competition than in each of the patches (Fig. 5c). As result, vegetation tends to disappear from these interpatch regions. Moreover, as vegetation dies in the region between patches, individuals within each of the patches experience weaker competition for resources, which effectively leads to a positive feedback that increases the biomass inside the patch and enhances the structure of the pattern [23,59]. This same mechanism has been suggested to drive the formation of clusters of competing species in the niche space [91–95], and explains why spectral analyses of the patterns developed by purely competitive nonlocal models identify a characteristic wavelength between q and $2q$.

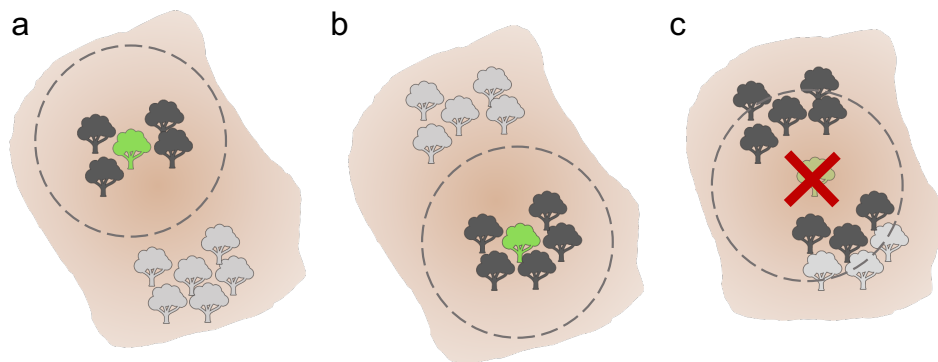


Figure 5. In kernel-based PC models, patchy distributions of vegetation in which the distance between patches is between one and two times the range of the nonlocal interactions are stable. Individuals within each patch only compete with the individuals in that patch (a,b), whereas individuals in between patches compete with individuals from both patches (c). Color code: green trees are focal individuals, and dashed circles limit the range of interaction of the focal individual. Dark grey is used for individuals that interact with the focal one, whereas light grey indicates individuals that are out of the range of interaction of the focal individual.

4. Self-organized patterns as indicators of ecological transitions

Models assuming different shapes for the net biotic interaction between neighbor plants have successfully reproduced qualitatively the spatial patterns of vegetation observed in water-limited ecosystems [13]. These different models also predict that the spotted pattern precedes a transition to an unvegetated state and thus could be used as early-warning indicators of ecological transitions [18,19]. However, models invoking different mechanisms to explain the formation of the same pattern can lead to very different desertification processes. As an example, we next revisit three different models for vegetation self-organization from previous sections and focus on their contradictory predictions about how ecosystems respond to aridification.

The Rietkerk model [21] (section 3.1.2) predicts that, if aridity keeps increasing after the system is in the spotted pattern, the ecosystem eventually collapses into a desert state following an abrupt transition that includes a hysteresis loop (Fig. 6a). Abrupt transitions such as this one are typical of bistable systems in which the stationary state depends on the environmental and the initial conditions. Bistability is a persistent feature of models for vegetation pattern formation, sometimes occurring also in transitions between patterned states [14], and it denotes thresholds in the system that trigger sudden, abrupt responses in its dynamics. These thresholds are often created by positive feedbacks or quorum-regulated behaviors as is the case in populations subject to strong Allee effects [96]. In the Rietkerk model, as rainfall decreases, the spatial distribution of vegetation moves through the gapped-labyrinthine-spotted sequence of patterns (Fig. 6a). However, when the rainfall crosses a threshold value ($R \approx 0.55 \text{ mm day}^{-1}$ for parameter values in Table 1 and using the initial condition in the caption of Fig. 6), the system responds abruptly, and all vegetation dies. Once the system reaches this unvegetated state, increasing water availability does not allow vegetation recovery until $R \approx 0.70 \text{ mm day}^{-1}$, which results in a hysteresis loop and a region of bistability ($R \in [0.55, 0.70]$ in Fig. 6a). Bistability and hysteresis loops make abrupt, sudden transitions like this one extremely hard to revert. Hence, anticipating such abrupt transitions is critical from a conservation and ecosystem-management point of view [18,19].

Extended versions of the Rietkerk model have suggested that the interaction between vegetation and other biotic components of the ecosystem may change the transition to the unvegetated state (see section 3.1.2). Specifically, Bonachela *et al.* [46] suggested that soil-dwelling termites, in establishing their

nests (mounds), engineer the chemical and physical properties of the soil in a way that turns the abrupt desertification into a two-step process (Fig. 6b). At a certain precipitation level ($R \approx 0.75 \text{ mm day}^{-1}$) using the parameterization in Table 1 and the same initial condition used for the original Rietkerk model), vegetation dies in most of the landscape (T1 in Fig. 6b) but persists on the mounds due to improved properties for plant growth created by the termites. On-mound vegetation survives even if precipitation continues to decline, and is finally lost at a rainfall threshold $R \approx 0.35 \text{ mm day}^{-1}$ (T2 in Fig. 6b). As a consequence of the two-step transition, the ecosystem collapse is easier to prevent because a bare soil matrix with vegetation only on mounds serves as an early-warning signal of desertification, and it is easier to revert since termite-induced heterogeneity breaks the large hysteresis loop of the original model into two smaller ones (compare the hysteresis loops in Fig. 6a and Fig. 6b).

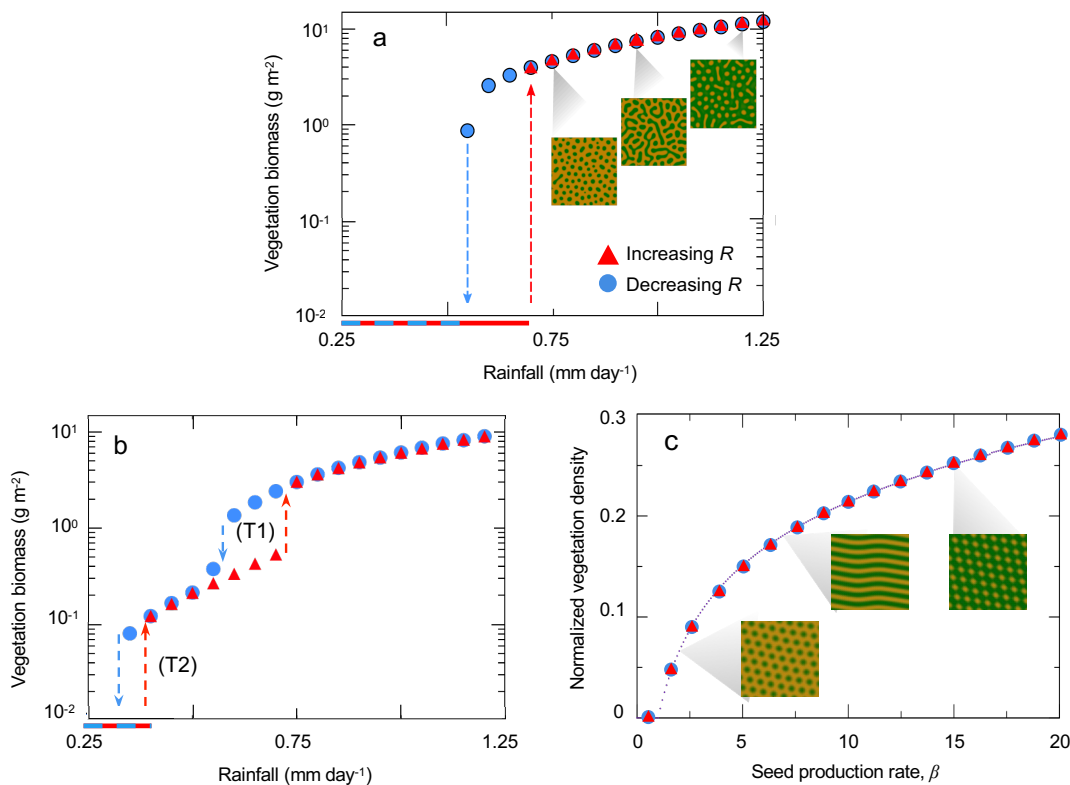


Figure 6. Although models for vegetation pattern formation may recover the same sequence of gapped-labyrinthine-spotted patterns from different mechanism, the type of desertification transition that follows the spotted pattern strongly depends on the model ingredients. a) Abrupt desertification as predicted by the Rietkerk model [21]. Simulations were conducted on a squared environment of lateral length 200m with discretization $\Delta x = \Delta y = 2\text{m}$ and using the model parameterization in Table 1. Simulations were started by introducing peaks of vegetation in 1% of the grid elements, which were all set in the unvegetated equilibrium. b) Two-step desertification process as predicted in Bonachela *et al.* [46] simulations were conducted using the same parameterization and initial condition used in panel a. c) Progressive desertification as predicted by the purely competitive model introduced in Martínez-García *et al.* [59]. Numerical simulations were conducted using the same setup described in Fig. (4).

Finally, the PC model with nonlinear nonlocal interactions of section 3.3.1 [59] predicts a smooth desertification in which vegetation biomass decreases continuously in response to decreasing seed production rate (a proxy for worsening environmental conditions). According to this model, the spotted

pattern would persist as precipitation declines, with vegetation biomass decreasing until it eventually disappears (Fig. 6c). As opposed to catastrophic shifts, smooth transitions such as the one depicted by this model do not show bistability and do not feature hysteresis loops. This difference has important socio-ecological implications because it enables easier and more affordable management strategies to restore the ecosystem after the collapse [61]. Moreover, continuous transitions are also more predictable because the density of vegetation is univocally determined by the control parameter (seed production rate β in Fig. 6c).

Therefore, patterns have tremendous potential for ecosystem management as an inexpensive and reliable early indicator of ecological transitions [18,19]. However, predictability requires the development of tailored models that reproduce observed patterns from the mechanisms relevant to the focal system. We have shown that widespread spotted patterns can form in models accounting for very different mechanisms (Fig. 6). Crucially, however, each of these models predicts a very different type of desertification transition. Because ecosystems are highly complex, it is very likely that spotted patterns observed in different regions emerge from very different mechanisms (or combinations of them) and thus anticipate transitions of very different natures. Therefore, a reliable use of spotted patterns as early warning indicators of ecosystem collapse requires a mix of (a) mechanistic models that are parameterized and validated by empirical observations of both mechanisms and patterns, (b) quantitative analyses of field observations, and (c) manipulative experiments.

5. Testing models for vegetation self-organization in the field

In this section, we discuss possible experimental approaches to test whether and which of the previously reviewed types of models is at play in a specific patterned ecosystem, which would help determine whether an eventual desertification transition is more likely to be abrupt or continuous.

The first step that we propose is to test the spatial distribution of the sign of the net interaction between plants. Only two net-interaction distributions have been theoretically predicted to produce spatial vegetation patterns. A PC distribution allows patterns to emerge from negative net interactions being ubiquitous. The classic SDF distribution generates similar patterns from positive interactions dominating under-canopy areas and negative interactions dominating bare-soil areas. A simple experimental setup, based on mainstream plant biotic interaction methodologies [97], would allow one to discern whether the PC or the SDF distribution of net interactions predominates in the focal ecosystem.

Our proposed experiment would compare a fitness proxy (e.g., growth, survival) for plants growing under-canopy (Fig. 7a) and in bare soil (Fig. 7b), to that of control plants growing in the same ecosystem but artificially isolated from the interaction with pattern-forming individuals (Fig. 7c). To isolate control plants from canopy interaction they need to be planted in bare soil areas. To isolate them from below-ground competition, one can excavate narrow, deep trenches in which a root barrier can be inserted [98]. The SDF hypothesis would be validated if a predominantly positive net interaction is observed under the canopy, and a negative interaction is observed in bare soils. Conversely, the PC hypothesis would be proved if a negative net interaction is observed in bare soils and under canopy (see Table 2). Any other outcome in the spatial distribution of the sign of the net interaction between plants would suggest that other mechanisms are at play, which could include the action of different ecosystem components, such as soil-dwelling macrofauna [44], or abiotic factors, such as micro-topology.

After discriminating between the PC and SDF hypotheses, a second experimental step would be to further explore the biophysical mechanisms responsible for the measured interaction (e.g., above and below-ground competition, soil or climate amelioration..) and driving the spatial pattern. These biophysical mechanisms can be complex, and some have been proposed as potential major drivers of vegetation self-organization [66]. For example, PC models hypothesize that spatial patterns are driven by

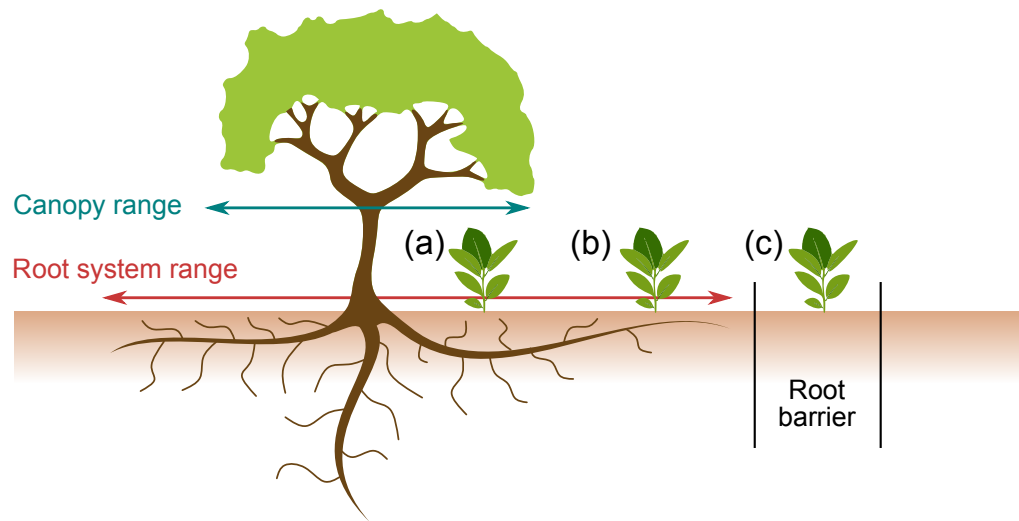


Figure 7. Schematic representation of a simple experimental setup to test in the field whether the mechanism of spatial patterning is purely competitive (PC) or a classic scale-dependent feedback (SDF). Plant (a) is an experimental plant growing under-canopy, (b) is growing in bare soil, and (c) is a control plant growing in artificial conditions, free from the biotic interaction using soil barriers in bare soil areas of the same environment.

Under canopy vs control	Bare soil vs control	Outcome
0/–	–	Purely competitive
+	–	Scale-dependent feedback

Table 2. Testing the PC versus SDF hypotheses in the experimental setup introduced in Fig. 7. Indexes to calculate the sign of the net interaction can be taken from Armas *et al.* [97].

long-range below-ground competition for a limiting resource through the formation of exclusion regions. As discussed in section 3.3.2, these exclusion regions are territories between patches of vegetation in which the intensity of competition is higher than within the patch [89], possibly because they present a higher density of roots (Fig. 5) [23,59]. To test for the existence of exclusion regions and confirm whether below-ground competition is driving the spatial pattern, researchers could measure root density across transects between two vegetated patches and through the bare soil.

Field tests and manipulative experiments to confirm that SDFs are responsible for vegetation patterns are not easy to perform. However, there are still a handful of analyses that researchers could do. For example, the Rietkerk SDF model [21] assumes that (i) water infiltration is significantly faster in vegetation patches than in bare soil areas and (ii) that surface water diffusion (i.e., runoff speed) is several orders of magnitude larger than vegetation diffusion (i.e., patch growth speed). To test the first assumption, researchers can use infiltrometers to quantify water infiltration rates in both vegetated patches and bare-soil areas [99,100]. This difference in water infiltration due to the presence of vegetation should also result in higher densities of water in the soil underneath vegetation patches than in the bare soil, which can be quantified using field moisture sensors [101]. To test the second assumption, field researchers need to measure the intensity of the water runoff and compare it with a measure of the lateral growth rate of vegetation patches. Water runoff is very challenging to measure directly, but reliable estimates can

be calculated using infiltration rates [102]. Note, however, that infiltration rates might be very hard to measure due to small-scale soil heterogeneities and expect water runoff estimates derived from them to be reliable only for a subset of ecosystems with more homogeneous soils. The lateral growth rate of vegetation patches can be estimated based on drone or satellite images repeated over time. Combining measures of both water runoff and expansion rates of vegetation patches, one can estimate approximated values for the relative ratio of the two metrics.

6. Conclusions and future lines of research

As our ability to obtain and analyze large, high-resolution images of the Earth's surface increases, more examples of self-organized vegetation patterns are found in water-limited ecosystems. Here, we have reviewed different modeling approaches employed to understand the mathematical origin and the predicted consequences of those patterns. We have shown that different models, relying on different mechanisms, can successfully reproduce the patterns observed in natural systems. However, each of these models predicts very different ecosystem-level consequences of the emergent pattern, which limits the utility of the patterns alone to be used as applied ecological tools in the absence of explicit knowledge of underlying mechanisms. To solve this issue, we claim that models need to move from their current universal but phenomenological formulation towards a more system-specific but mechanistic one, focused on isolating the system-specific, key feedbacks for vegetation self-organization. To this end, we identify several directions for future research.

First, biologically-grounded studies should aim to combine system-specific models with empirical measures of vegetation-mediated feedbacks. Existing models for vegetation self-organization are mostly phenomenological and are only validated qualitatively via the visual comparison of simulated and observed (macroscopic) patterns. Experimental measures of the (microscopic) processes and feedbacks central to most models of vegetation pattern formation are hard to obtain, leading to arbitrary (free) parameter values and response functions. For example, very few models incorporate empirically-validated values of water diffusion and plant dispersal rates, despite the crucial role of these parameters in the emergence of patterns. Instead, these models fine-tune such values to obtain patterns similar in, for example, their wavelength, to the natural pattern. Similarly we are only beginning to understand how plants rearrange their root system in the presence of competing individuals [103], and hence kernel-based models do not incorporate realistic functional forms for the kernels. Instead, these models use phenomenological functions to test potential mechanisms for pattern formation by qualitatively comparing model output and target pattern, thus limiting the potential of the models to make quantitative predictions.

PDEMs are analytically more tractable than IBMs and enable the identification of processes that trigger the instabilities responsible for the patterns [9]. However, such PDEMs only have true predictive power if derived from the correct microscopic dynamics and properly parameterized via system-specific measures. Thus, in order to establish a dialogue between experiments and theory, models should develop from a microscopic description of the system [27,28] that allows for a more realistic and accurate description of the plant-to-plant and plant-water interactions, as well as for a better reconciliation between model parameters and system-specific empirical measures. Subsequently, existing tools from mathematics, statistical physics, and/or computer science can be used to reach a macroscopic PDEM that captures the key ingredients of the microscopic dynamics. Statistical physics, which was conceived to describe how observed macroscopic properties of physical systems emerge from the underlying microscopic processes, provides a compelling and well-developed framework to make such a micro-macro connection.

Second, recent developments in remotely sensed imagery have enabled the measurement of an ecosystem's state indicators, which will allow researchers to compare observed and simulated patterns quantitatively [25]. On the one hand, using existing databases of ecosystem responses to aridity [65]

and satellite imagery of vegetation coverage [13], researchers could conduct a model selection analysis and classify existing models from more to less realistic depending on whether (and how many) features of the focal ecosystem the model manages to reproduce in the correct environmental conditions. For example, models could be classified depending on whether, after proper parameterization, they can predict ecosystem responses such as transitions between pattern types at the correct aridity thresholds. To elaborate this model classification, the use of Fourier analysis for identifying regularity in natural patterns, geostatistics for quantifying spatial correlations, and time series analysis for tracking changes in the ecosystem properties through time will be essential. On the other hand, once we accumulate a long-term database of satellite images of the Earth's surface, researchers will be able to calculate the correlation between pattern shape and mean annual rainfall for a fixed location through time. This analysis will provide a more robust test for model predictions on the correlation between water availability and pattern type than existing ones using satellite images taken at different locations at the same time [13] because they will ensure that all model parameters except the mean annual rainfall are constant.

Finally, theoretical research should try to reconcile reaction-diffusion and kernel-based models. Despite recent efforts [23], the link between the two approaches is still lacking, making it hard to build biologically-meaningful kernels. To the best of our knowledge, any attempt to derive a kernel-based model starting from a water-vegetation reaction-diffusion model has been unsuccessful in reproducing a kernel shape that generates patterns. Only very few exceptions exist for certain approximations of kernel-based models with SDFs in which the nonlocal term is expanded into a series of differential operators [12]. We propose that the micro-macro scaling techniques discussed above can also help shed light on this question.

Beyond water-limited ecosystems, both SDF and competition/repulsion alone have been reported as drivers of spatial self-organization in many other biological and physical systems. A combination of attractive and repulsive forces acting on different scales is, for instance, believed to be responsible for the formation of regular stripes in mussel beds [11]. Other models that investigate the formation of different structures in animal groupings also rely on similar attraction-repulsion or activation-inhibition principles [104–109]. On the other hand, several biological systems also self-organize only as a consequence of repulsive or growth-inhibitory interactions alone. For instance, territorial species and central-place foragers often create a hexagonal, overdispersed pattern of territory packing [44,110–112] (see [5] for a comprehensive review). Species in communities driven by competition have also been predicted to form clumps through the niche space [91,92,94,113] and long-range competition has been recently suggested as a potentially stabilizing mechanism in two-species communities [114]. In physical systems, cluster crystals form in some molecules and colloids that interact via effective repulsive forces [115–118]. Patterning in these disparate systems shares common properties: competition induces a hexagonal distribution of the clusters, and the transition to patterns is mathematically controlled by the sign of the Fourier transform of the kernel function, which indicates how quickly the intensity of the competition decays with the distance between individuals [59,117,119]. Understanding the conditions under which repulsion dominates attraction (or inhibition dominates activation) and finding the key features that distinguish the patterns that emerge in each of these scenarios across physical systems and different levels of biological organization constitutes another important line for future research.

Acknowledgments: We acknowledge Robert M. Pringle, Rubén Juanes, and Ignacio Rodríguez-Iturbe for various discussions at different stages of the development of this work

Author Contributions: “Conceptualization, R.M.G., C.C., J.A.B., J.M.C., E.H.G., C.L., C.E.T.; writing–original draft preparation, R.M.G.; writing–review and editing, R.M.G., C.C., J.A.B., J.M.C., E.H.G., C.L., C.E.T.; visualization, R.M.G., C.C. All authors have read and agreed to the published version of the manuscript.”

Funding: “RMG: FAPESP through grants ICTP-SAIIR 2016/01343-7, and Programa Jovens Pesquisadores em Centros Emergentes 2019/24433-0 and 2019/05523-8, Instituto Serrapilheira through grant Serra-1911-31200, and the Simons Foundation. CC: the Princeton University May Fellowship in the department of Ecology and Evolutionary Biology.

JMC: Center of Advanced Systems Understanding (CASUS) which is financed by Germany's Federal Ministry of Education and Research (BMBF) and by the Saxon Ministry for Science, Culture and Tourism (SMWK) with tax funds on the basis of the budget approved by the Saxon State Parliament. EHG and CL: MINECO/AEI/FEDER through the María de Maeztu Program for Units of Excellence in R&D (MDM-2017-0711, Spain). CET & JAB acknowledge support from the Gordon and Betty Moore Foundation, grant #7800.

Conflicts of Interest: The authors declare no conflict of interest.

References

- Gregor, T.; Fujimoto, K.; Masaki, N.; Sawai, S. The onset of collective behavior in social amoebae. *Science (New York, N.Y.)* **2010**, *328*, 1021–5. doi:10.1126/science.1183415.
- Bonachela, J.A.; Nadell, C.D.; Xavier, J.B.; Levin, S.A. Universality in Bacterial Colonies. *Journal of Statistical Physics* **2011**, *144*, 303–315, [1108.1937]. doi:10.1007/s10955-011-0179-x.
- Martínez-García, R.; Nadell, C.D.; Hartmann, R.; Drescher, K.; Bonachela, J.A. Cell adhesion and fluid flow jointly initiate genotype spatial distribution in biofilms. *PLOS Computational Biology* **2018**, *14*, e1006094. doi:10.1371/journal.pcbi.1006094.
- Rietkerk, M.; van de Koppel, J. Regular pattern formation in real ecosystems. *Trends in ecology & evolution* **2008**, *23*, 169–175.
- Pringle, R.M.; Tarnita, C.E. Spatial Self-Organization of Ecosystems: Integrating Multiple Mechanisms of Regular-Pattern Formation. *Annual Review of Entomology* **2017**, *62*, 359–377. doi:10.1146/annurev-ento-031616-035413.
- Meinhardt, H. Models of biological pattern formation. *New York* **1982**, p. 118.
- Camazine, S.; Deneubourg, J.L.; Franks, N.R.; Sneyd, J.; Bonabeau, E.; Theraula, G. *Self-organization in biological systems*; Princeton university press, 2003.
- Sole, R.V.; Bascompte, J. *Self-organization in complex ecosystems*; Princeton University Press, 2006; p. 373.
- Meron, E. From Patterns to Function in Living Systems: Dryland Ecosystems as a Case Study. *Annual Review of Condensed Matter Physics* **2018**, *9*, 79–103. doi:10.1146/annurev-conmatphys-033117-053959.
- Deblauwe, V.; Barbier, N.; Couteron, P.; Lejeune, O.; Bogaert, J. The global biogeography of semi-arid periodic vegetation patterns. *Global Ecology and Biogeography* **2008**, *17*, 715–723. doi:10.1111/j.1466-8238.2008.00413.x.
- Rietkerk, M.; van de Koppel, J. Regular pattern formation in real ecosystems. *Trends in ecology & evolution* **2008**, *23*, 169–175.
- Borgogno, F.; D'Odorico, P.; Laio, F.; Ridolfi, L. Mathematical models of vegetation pattern formation in ecohydrology. *Reviews of Geophysics* **2009**, *47*. doi:10.1029/2007rg000256.
- Deblauwe, V.; Couteron, P.; Lejeune, O.; Bogaert, J.; Barbier, N. Environmental modulation of self-organized periodic vegetation patterns in Sudan. *Ecography* **2011**, *34*, 990–1001.
- von Hardenberg, J.; Meron, E.; Shachak, M.; Zarmi, Y. Diversity of Vegetation Patterns and Desertification. *Physical Review Letters* **2001**, *87*. doi:10.1103/physrevlett.87.198101.
- Meron, E.; Gilad, E.; von Hardenberg, J.; Shachak, M.; Zarmi, Y. Vegetation patterns along a rainfall gradient. *Chaos, Solitons & Fractals* **2004**, *19*, 367–376. doi:10.1016/s0960-0779(03)00049-3.
- Scheffer, M.; Carpenter, S.R. Catastrophic regime shifts in ecosystems: linking theory to observation. *Trends in Ecology & Evolution* **2003**, *18*, 648–656. doi:10.1016/j.tree.2003.09.002.
- Rietkerk, M.; Dekker, S.C.; De Ruiter, P.C.; van de Koppel, J. Self-organized patchiness and catastrophic shifts in ecosystems. *Science* **2004**, *305*, 1926–9. doi:10.1126/science.1101867.
- Scheffer, M.; Bascompte, J.; Brock, W.A.; Brovkin, V.; Carpenter, S.R.; Dakos, V.; Held, H.; van Nes, E.H.; Rietkerk, M.; Sugihara, G. Early-warning signals for critical transitions. *Nature* **2009**, *461*, 53–9. doi:10.1038/nature08227.
- Dakos, V.; Kéfi, S.; Rietkerk, M.; Van Nes, E.H.; Scheffer, M. Slowing down in spatially patterned ecosystems at the brink of collapse. *The American Naturalist* **2011**, *177*, E153–E166.
- Dakos, V.; Carpenter, S.R.; van Nes, E.H.; Scheffer, M. Resilience indicators: prospects and limitations for early warnings of regime shifts. *Philosophical Transactions of the Royal Society B: Biological Sciences* **2015**, *370*, 20130263.

21. Rietkerk, M.; Boerlijst, M.C.; van Langevelde, F.; HilleRisLambers, R.; van de Koppel, J.; Kumar, L.; Prins, H.H.T.; de Roos, A.M. Self-Organization of Vegetation in Arid Ecosystems. *The American Naturalist* **2002**, *160*, 524–530. doi:10.1086/342078.
22. Meron, E.; Gilad, E.; Von Hardenberg, J.; Shachak, M.; Zarmi, Y. Vegetation patterns along a rainfall gradient. *Chaos, Solitons and Fractals* **2004**, *19*, 367–376. doi:10.1016/S0960-0779(03)00049-3.
23. Martínez-García, R.; Calabrese, J.M.; Hernández-García, E.; López, C. Minimal mechanisms for vegetation patterns in semiarid regions. *Philosophical Transactions of the Royal Society A: Mathematical, Physical and Engineering Sciences* **2014**, *372*, 20140068. doi:10.1098/rsta.2014.0068.
24. Gowda, K.; Riecke, H.; Silber, M. Transitions between patterned states in vegetation models for semiarid ecosystems. *Physical Review E* **2014**, *89*, 022701. doi:10.1103/PhysRevE.89.022701.
25. Bastiaansen, R.; Jaïbi, O.; Deblauwe, V.; Eppinga, M.B.; Siteur, K.; Siero, E.; Mermoz, S.; Bouvet, A.; Doelman, A.; Rietkerk, M. Multistability of model and real dryland ecosystems through spatial self-organization. *Proceedings of the National Academy of Sciences* **2018**, *115*, 11256–11261.
26. Herben, T.; Hara, T., Spatial Pattern Formation in Plant Communities. In *Morphogenesis and Pattern Formation in Biological Systems: Experiments and Models*; Sekimura, T.; Noji, S.; Ueno, N.; Maini, P.K., Eds.; Springer Japan: Tokyo, 2003; pp. 223–235. doi:10.1007/978-4-431-65958-7_19.
27. Railsback, S.F.; Grimm, V. *Agent-based and individual-based modeling: a practical introduction*; Princeton university press, 2019.
28. DeAngelis, D.L.; Yurek, S. Spatially Explicit Modeling in Ecology: A Review. *Ecosystems* **2016**, *20*, 284–300. doi:10.1007/s10021-016-0066-z.
29. Meron, E. *Nonlinear physics of ecosystems*; CRC Press, 2015.
30. Meron, E.; Bennett, J.J.; Fernandez-Oto, C.; Tzuk, O.; Zelnik, Y.R.; Grafi, G. Continuum Modeling of Discrete Plant Communities: Why Does It Work and Why Is It Advantageous? *Mathematics* **2019**, *7*, 987.
31. Matsuda, H.; Ogita, N.; Sasaki, A.; Sato, K. Statistical Mechanics of Population: The Lattice Lotka-Volterra Model. *Progress of Theoretical Physics* **1992**, *88*, 1035–1049. doi:10.1143/ptp/88.6.1035.
32. Bolker, B.M.; Pacala, S.W. Using moment equations to understand stochastically driven spatial pattern formation in ecological systems. *Theoretical Population Biology* **1997**, *52*, 179–197. doi:10.1006/tpbi.1997.1331.
33. Bolker, B.M.; Pacala, S.W. Spatial moment equations for plant competition: Understanding spatial strategies and the advantages of short dispersal. *American Naturalist* **1999**, *153*, 575–602. doi:10.1086/303199.
34. Ellner, S.P. Pair approximation for lattice models with multiple interaction scales. *Journal of theoretical biology* **2001**, *210*, 435–47. doi:10.1006/jtbi.2001.2322.
35. Law, R.; Murrell, D.J.; Dieckmann, U. Population growth in space and time: spatial logistic equations. *Ecology* **2003**, *84*, 252–262.
36. Calabrese, J.M.; Vazquez, F.; López, C.; San Miguel, M.; Grimm, V. The independent and interactive effects of tree-tree establishment competition and fire on savanna structure and dynamics. *The American Naturalist* **2010**, *175*, E44–65. doi:10.1086/650368.
37. Iwasa, Y. Lattice Models and Pair Approximation in Ecology. In *The Geometry of Ecological Interactions*; Dieckmann, U.; Law, R.; Metz, J., Eds.; Cambridge University Press: Cambridge, 2010; chapter 13, pp. 227–251. doi:10.1017/cbo9780511525537.016.
38. Plank, M.J.; Law, R. Spatial point processes and moment dynamics in the life sciences: a parsimonious derivation and some extensions. *Bulletin of mathematical biology* **2015**, *77*, 586–613.
39. Surendran, A.; Plank, M.; Simpson, M. Population dynamics with spatial structure and an Allee effect. *bioRxiv* **2020**.
40. Cross, M.C.; Hohenberg, P. Pattern formation outside of equilibrium. *Reviews of Modern Physics* **1993**, *65*.
41. Klausmeier, C.A. Regular and Irregular Patterns in Semiarid Vegetation. *Science* **1999**, *284*, 1826–1828. doi:10.1126/science.284.5421.1826.
42. Eigentler, L. Intraspecific competition in models for vegetation patterns: Decrease in resilience to aridity and facilitation of species coexistence. *Ecological Complexity* **2020**, *42*. doi:10.1016/j.ecocom.2020.100835.

43. Gilad, E.; von Hardenberg, J.; Provenzale, A.; Shachak, M.; Meron, E. Ecosystem Engineers: From Pattern Formation to Habitat Creation. *Physical Review Letters* **2004**, *93*, 098105. doi:10.1103/PhysRevLett.93.098105.
44. Tarnita, C.E.; Bonachela, J.A.; Sheffer, E.; Guyton, J.A.; Coverdale, T.C.; Long, R.A.; Pringle, R.M. A theoretical foundation for multi-scale regular vegetation patterns. *Nature* **2017**, *541*, 398–401. doi:10.1038/nature20801.
45. Marasco, A.; Iuorio, A.; Cartení, F.; Bonanomi, G.; Tartakovsky, D.M.; Mazzoleni, S.; Giannino, F. Vegetation Pattern Formation Due to Interactions Between Water Availability and Toxicity in Plant–Soil Feedback. *Bulletin of Mathematical Biology* **2014**, *76*, 2866–2883. doi:10.1007/s11538-014-0036-6.
46. Bonachela, J.A.; Pringle, R.M.; Sheffer, E.; Coverdale, T.C.; Guyton, J.A.; Caylor, K.K.; Levin, S.A.; Tarnita, C.E. Termite mounds can increase the robustness of dryland ecosystems to climatic change. *Science* **2015**, *347*, 651–655. doi:10.1126/science.1261487.
47. Iuorio, A.; Veerman, F. The influence of autotoxicity on the dynamics of vegetation spots. *bioRxiv* **2020**, pp. 1–27. doi:doi.org/10.1101/2020.07.29.226522 .
48. Berghuis, P.M.; Mayor, Á.G.; Rietkerk, M.; Baudena, M. More is not necessarily better: The role of cover and spatial organization of resource sinks in the restoration of patchy drylands. *Journal of Arid Environments* **2020**, *183*. doi:10.1016/j.jaridenv.2020.104282.
49. Gandhi, P.; Werner, L.; Iams, S.; Gowda, K.; Silber, M. A topographic mechanism for arcing of dryland vegetation bands. *Journal of The Royal Society Interface* **2018**, *15*, 20180508. doi:10.1098/rsif.2018.0508.
50. Porporato, A.; D’odorico, P.; Laio, F.; Ridolfi, L.; Rodriguez-Iturbe, I. Ecohydrology of water-controlled ecosystems. *Advances in Water Resources* **2002**, *25*, 1335–1348.
51. Porporato, A.; Daly, E.; Rodriguez-Iturbe, I. Soil water balance and ecosystem response to climate change. *The American Naturalist* **2004**, *164*, 625–632.
52. Rodríguez-Iturbe, I.; Isham, V.; Cox, D.R.; Manfreda, S.; Porporato, A. Space-time modeling of soil moisture: Stochastic rainfall forcing with heterogeneous vegetation. *Water Resources Research* **2006**, *42*, 1–11. doi:10.1029/2005WR004497.
53. D’Odorico, P.; Laio, F.; Ridolfi, L. Vegetation patterns induced by random climate fluctuations. *Geophysical Research Letters* **2006**, *33*. doi:10.1029/2006gl027499.
54. De Michele, C.; Vezzoli, R.; Pavlopoulos, H.; Scholes, R. A minimal model of soil water–vegetation interactions forced by stochastic rainfall in water-limited ecosystems. *Ecological Modelling* **2008**, *212*, 397–407.
55. Ridolfi, L.; D’Odorico, P.; Laio, F. *Noise-induced phenomena in the environmental sciences*; Cambridge University Press, 2011.
56. Eigentler, L.; Sherratt, J.A. Effects of precipitation intermittency on vegetation patterns in semi-arid landscapes. *Physica D: Nonlinear Phenomena* **2020**, *405*, 132396, [1911.10878]. doi:10.1016/j.physd.2020.132396.
57. Martínez-García, R.; Calabrese, J.M.; López, C. Spatial patterns in mesic savannas: The local facilitation limit and the role of demographic stochasticity. *Journal of Theoretical Biology* **2013**, *333*, 156–165. doi:10.1016/j.jtbi.2013.05.024.
58. Butler, T.; Goldenfeld, N. Robust ecological pattern formation induced by demographic noise. *Physical Review E* **2009**, *80*. doi:10.1103/physreve.80.030902.
59. Martínez-García, R.; Calabrese, J.M.; Hernández-García, E.; López, C. Vegetation pattern formation in semiarid systems without facilitative mechanisms. *Geophysical Research Letters* **2013**, *40*, 6143–6147. doi:10.1002/2013gl058797.
60. Mortimore, M.; Anderson, S.; Cotula, L.; Davies, J.; Facer, K.; Hesse, C.; Morton, J.; Nyangena, W.; Skinner, J.; Wolfangel, C. Dryland Opportunities: A new paradigm for people, ecosystems and development. Technical report, International Union for Conservation of Nature (IUCN), 2009.
61. Villa Martín, P.; Bonachela, J.A.; Levin, S.A.; Muñoz, M.Á. Eluding catastrophic shifts. *Proceedings of the National Academy of Sciences* **2015**, *112*, E1828–E1836. doi:10.1073/pnas.1414708112.
62. Conde-Pueyo, N.; Vidiella, B.; Sardanyés, J.; Berdugo, M.; Maestre, F.T.; de Lorenzo, V.; Solé, R. Synthetic biology for terraformation lessons from mars, earth, and the microbiome. *Life* **2020**, *10*, 1–27. doi:10.3390/life10020014.
63. Vidiella, B.; Sardanyés, J.; Solé, R. Synthetic soil crusts against green-desert transitions: a spatial model. *Royal Society Open Science* **2020**, *7*, 200161. doi:10.1101/838631.

64. Maestre, F.T.; Eldridge, D.J.; Soliveres, S.; Kéfi, S.; Delgado-Baquerizo, M.; Bowker, M.A.; García-Palacios, P.; Gaitán, J.; Gallardo, A.; Lázaro, R.; Berdugo, M. Structure and Functioning of Dryland Ecosystems in a Changing World. *Annual Review of Ecology, Evolution, and Systematics* **2016**, *47*, 215–237. doi:10.1146/annurev-ecolsys-121415-032311.
65. Berdugo, M.; Delgado-Baquerizo, M.; Soliveres, S.; Hernández-Clemente, R.; Zhao, Y.; Gaitán, J.J.; Gross, N.; Saiz, H.; Maire, V.; Lehman, A.; Rillig, M.C.; Solé, R.V.; Maestre, F.T. Global ecosystem thresholds driven by aridity. *Science* **2020**, *367*, 787–790. doi:10.1126/science.aay5958.
66. Cabal, C.; Martínez-García, R.; Valladares, F. The ecology of plant interactions: A giant with feet of clay. *Preprints* **2020**, p. 2020090520. doi:10.20944/preprints202009.0520.v1.
67. Valladares, F.; Laanisto, L.; Niinemets, Ü.; Zavala, M.A. Shedding light on shade: ecological perspectives of understorey plant life. *Plant Ecology and Diversity* **2016**, *9*, 237–251. doi:10.1080/17550874.2016.1210262.
68. Ludwig, F.; De Kroon, H.; Berendse, F.; Prins, H.H. The influence of savanna trees on nutrient, water and light availability and the understorey vegetation. *Plant Ecology* **2004**, *97*, 199–205. doi:10.1023/B:VEGE.0000019023.29636.92.
69. Montaña, C. The Colonization of Bare Areas in Two-Phase Mosaics of an Arid Ecosystem. *The Journal of Ecology* **1992**, *80*, 315–327. doi:10.2307/2261014.
70. Bromley, J.; Brouwer, J.; Barker, A.P.; Gaze, S.R.; Valentin, C. The role of surface water redistribution in an area of patterned vegetation in a semi-arid environment, south-west Niger. *Journal of Hydrology* **1997**, *198*, 1–29. doi:10.1016/S0022-1694(96)03322-7.
71. Trautz, A.C.; Illangasekare, T.H.; Rodriguez-Iturbe, I. Role of co-occurring competition and facilitation in plant spacing hydrodynamics in water-limited environments. *Proceedings of the National Academy of Sciences* **2017**, *114*, 9379–9384. doi:10.1073/pnas.1706046114.
72. Craine, J.M.; Dybzinski, R. Mechanisms of plant competition for nutrients, water and light. *Functional Ecology* **2013**, *27*, 833–840. doi:10.1111/1365-2435.12081.
73. Turing, A.M. The chemical basis of morphogenesis. *Philosophical Transactions of the Royal Society of London. Series B, Biological Sciences* **1952**, *237*, 37–72. doi:10.1007/BF02459572.
74. HilleRisLambers, R.; Rietkerk, M.; van den Bosch, F.; Prins, H.H.T.; de Kroon, H. Vegetation Pattern Formation in Semi-Arid Grazing Systems. *Ecology* **2001**, *82*, 50. doi:10.2307/2680085.
75. Meron, E. Pattern formation – A missing link in the study of ecosystem response to environmental changes. *Mathematical Biosciences* **2016**, *271*, 1–18. doi:10.1016/j.mbs.2015.10.015.
76. Kealy, B.J.; Wollkind, D.J. A Nonlinear Stability Analysis of Vegetative Turing Pattern Formation for an Interaction–Diffusion Plant–Surface Water Model System in an Arid Flat Environment. *Bulletin of Mathematical Biology* **2011**, *74*, 803–833. doi:10.1007/s11538-011-9688-7.
77. Gowda, K.; Chen, Y.; Iams, S.; Silber, M. Assessing the robustness of spatial pattern sequences in a dryland vegetation model. *Proceedings of the Royal Society A: Mathematical, Physical and Engineering Sciences* **2016**, *472*. doi:10.1098/rspa.2015.0893.
78. Salem, B.; others. *Arid zone forestry: a guide for field technicians.*; Number 20, Food and Agriculture Organization (FAO), 1989.
79. Kletter, A.Y.; von Hardenberg, J.; Meron, E.; Provenzale, A. Patterned vegetation and rainfall intermittency. *Journal of Theoretical Biology* **2009**, *256*, 574–583. doi:10.1016/j.jtbi.2008.10.020.
80. D’Odorico, P.; Laio, F.; Ridolfi, L. Patterns as indicators of productivity enhancement by facilitation and competition in dryland vegetation. *Journal of Geophysical Research* **2006**, *111*. doi:10.1029/2006jg000176.
81. Murray, J. *Mathematical biology. Vol II.*; Vol. 18, Springer, 2002.
82. Gerstner, W.; Kistler, W.M.; Naud, R.; Paninski, L. *Neuronal dynamics: From single neurons to networks and models of cognition*; Cambridge University Press, 2014.
83. Lefever, R.; Lejeune, O. On the origin of tiger bush. *Bulletin of Mathematical Biology* **1997**, *59*, 263–294. doi:10.1007/bf02462004.

84. Fernandez-Oto, C.; Tlidi, M.; Escaff, D.; Clerc, M.G. Strong interaction between plants induces circular barren patches: fairy circles. *Philosophical Transactions of the Royal Society A: Mathematical, Physical and Engineering Sciences* **2014**, *372*, 20140009. doi:10.1098/rsta.2014.0009.
85. Escaff, D.; Fernandez-Oto, C.; Clerc, M.G.; Tlidi, M. Localized vegetation patterns, fairy circles, and localized patches in arid landscapes. *Physical Review E* **2015**, *91*. doi:10.1103/physreve.91.022924.
86. Berríos-Caro, E.; Clerc, M.; Escaff, D.; Sandivari, C.; Tlidi, M. On the repulsive interaction between localised vegetation patches in scarce environments. *Scientific Reports* **2020**, *10*, 1–8.
87. Parra-Rivas, P.; Fernandez-Oto, C. Formation of localized states in dryland vegetation: Bifurcation structure and stability. *Physical Review E* **2020**, *101*, 052214.
88. Barbier, N.; Couteron, P.; Lefever, R.; Deblauwe, V.; Lejeune, O. Spatial decoupling of facilitation and competition at the origin of gapped vegetation patterns. *Ecology* **2008**, *89*, 1521–1531. doi:10.1890/07-0365.1.
89. van de Koppel, J.; Crain, C.M. Scale-Dependent Inhibition Drives Regular Tussock Spacing in a Freshwater Marsh. *The American Naturalist* **2006**, *168*, E136–E147. doi:10.1086/508671.
90. van de Koppel, J.; Gascoigne, J.C.; Theraulaz, G.; Rietkerk, M.; Mooij, W.M.; Herman, P.M. Experimental evidence for spatial self-organization and its emergent effects in mussel bed ecosystems. *Science* **2008**, *322*, 739–42. doi:10.1126/science.1163952.
91. Scheffer, M.; van Nes, E.H. Self-organized similarity, the evolutionary emergence of groups of similar species. *Proceedings of the National Academy of Sciences of the United States of America* **2006**, *103*, 6230–5. doi:10.1073/pnas.0508024103.
92. Pigolotti, S.; López, C.; Hernández-García, E. Species Clustering in Competitive Lotka-Volterra Models. *Physical Review Letters* **2007**, *98*, 258101.
93. Hernández-García, E.; López, C.; Pigolotti, S.; Andersen, K.H. Species competition: coexistence, exclusion and clustering. *Philosophical transactions. Series A, Mathematical, physical, and engineering sciences* **2009**, *367*, 3183–95. doi:10.1098/rsta.2009.0086.
94. Fort, H.; Scheffer, M.; van Nes, E.H. The paradox of the clumps mathematically explained. *Theoretical Ecology* **2009**, *2*, 171–176.
95. Leimar, O.; Sasaki, A.; Doebeli, M.; Dieckmann, U. Limiting similarity, species packing, and the shape of competition kernels. *Journal of Theoretical Biology* **2013**, *339*, 3 – 13. doi:https://doi.org/10.1016/j.jtbi.2013.08.005.
96. Courchamp, F.; Clutton-Brock, T.; Grenfell, B. Inverse density dependence and the Allee effect. *Trends in ecology & evolution* **1999**, *14*, 405–410.
97. Armas, C.; Ordiales, R.; Pugnaire, F.I. Measuring plant interactions: a new comparative index. *Ecology* **2004**, *85*, 2682–2686.
98. Morgenroth, J. A review of root barrier research. *Arboriculture and Urban Forestry* **2008**, *34*, 84–88.
99. Gregory, J.H.; Dukes, M.D.; Miller, G.L.; Jones, P.H. Analysis of double-ring infiltration techniques and development of a simple automatic water delivery system. *Applied Turfgrass Science* **2005**, *2*, 1–7.
100. Cramer, M.D.; Barger, N.N.; Tschinkel, W.R. Edaphic properties enable facilitative and competitive interactions resulting in fairy circle formation. *Ecography* **2017**, *40*, 1210–1220. doi:10.1111/ecog.02461.
101. Scheberl, L.; Scharenbroch, B.C.; Werner, L.P.; Prater, J.R.; Fite, K.L. Evaluation of soil pH and soil moisture with different field sensors: Case study urban soil. *Urban Forestry & Urban Greening* **2019**, *38*, 267–279.
102. Cook, H.L. The infiltration approach to the calculation of surface runoff. *Eos, Transactions American Geophysical Union* **1946**, *27*, 726–747.
103. Cabal, C.; Martínez-García, R.; De Castro, A.; Valladares, F.; Pacala, S.W. The Exploitative Segregation of Plant Roots. *Science* **2020**, *1199*, 1197–1199.
104. Couzin, I.D.; Krause, J.; James, R.; Ruxton, G.D.; Franks, N.R. Collective Memory and Spatial Sorting in Animal Groups. *Journal of Theoretical Biology* **2002**, *218*, 1–11. doi:10.1006/jtbi.2002.3065.
105. Couzin, I.D.; Krause, J. Self-Organization and Collective Behavior in Vertebrates. In *Advances in the Study of Behavior*; Elsevier, 2003; pp. 1–75. doi:10.1016/s0065-3454(03)01001-5.

106. Martínez-García, R.; Murgui, C.; Hernández-García, E.; López, C. Pattern Formation in Populations with Density-Dependent Movement and Two Interaction Scales. *PLOS ONE* **2015**, *10*, e0132261. doi:10.1371/journal.pone.0132261.
107. Liu, Q.X.; Doelman, A.; Rottschäfer, V.; de Jager, M.; Herman, P.M.J.; Rietkerk, M.; van de Koppel, J. Phase separation explains a new class of self-organized spatial patterns in ecological systems. *Proceedings of the National Academy of Sciences* **2013**, *110*, 11905–11910. doi:10.1073/pnas.1222339110.
108. Liu, Q.X.; Rietkerk, M.; Herman, P.M.; Piersma, T.; Fryxell, J.M.; van de Koppel, J. Phase separation driven by density-dependent movement: A novel mechanism for ecological patterns. *Physics of Life Reviews* **2016**, *19*, 107–121. doi:10.1016/j.plrev.2016.07.009.
109. Vicsek, T.; Zafeiris, A. Collective motion. *Physics Reports* **2012**, *517*, 71–140.
110. Barlow, G.W. Hexagonal territories. *Animal Behaviour* **1974**, *22*, 876–IN1.
111. Peters, R.P.; Mech, L.D. Scent-marking in wolves: radio-tracking of wolf packs has provided definite evidence that olfactory sign is used for territory maintenance and may serve for other forms of communication within the pack as well. *American Scientist* **1975**, *63*, 628–637.
112. Doncaster, C.P.; Macdonald, D.W. Drifting territoriality in the red fox *Vulpes vulpes*. *The Journal of Animal Ecology* **1991**, pp. 423–439.
113. Segura, A.M.; Kruk, C.; Calliari, D.; García-Rodríguez, F.; Conde, D.; Widdicombe, C.E.; Fort, H. Competition drives clumpy species coexistence in estuarine phytoplankton. *Scientific Reports* **2013**, *3*, 1–6. doi:10.1038/srep01037.
114. Maciel, G.A.; Martínez-García, R. Enhanced species coexistence in Lotka-Volterra competition models due to nonlocal interactions **2020**. [[arXiv:q-bio.PE/2012.06249](https://arxiv.org/abs/2012.06249)].
115. Mladek, B.M.; Gottwald, D.; Kahl, G.; Neumann, M.; Likos, C.N. Formation of Polymorphic Cluster Phases for a Class of Models of Purely Repulsive Soft Spheres. *Physical Review Letters* **2006**, *96*. doi:10.1103/physrevlett.96.045701.
116. Likos, C.N.; Mladek, B.M.; Gottwald, D.; Kahl, G. Why do ultrasoft repulsive particles cluster and crystallize? Analytical results from density-functional theory. *The Journal of Chemical Physics* **2007**, *126*, 224502. doi:10.1063/1.2738064.
117. Delfau, J.B.; Ollivier, H.; López, C.; Blasius, B.; Hernández-García, E. Pattern formation with repulsive soft-core interactions: Discrete particle dynamics and Dean-Kawasaki equation. *Physical Review E* **2016**, *94*. doi:10.1103/physreve.94.042120.
118. Caprini, L.; Hernández-García, E.; López, C. Cluster crystals with combined soft- and hard-core repulsive interactions. *Phys. Rev. E* **2018**, *98*, 052607. doi:10.1103/PhysRevE.98.052607.
119. Hernández-García, E.; López, C. Birth, death and diffusion of interacting particles. *Journal of Physics: Condensed Matter* **2005**, *17*, S4263.